CZ9726685

SPECTROSCOPIC TECHNIQUES FOR MEASURING ION DIODE SPACE-CHARGE DISTRIBUTIONS AND ION SOURCE PROPERTIES

A.B. Filuk, J.E. Bailey, R.G. Adams, A.L. Carlson, C.-H. Ching, M.P. Desjarlais, P. Lake, E.J. McGuire, T.A. Mehlhorn, T.D. Pointon
Sandia National Laboratories, Albuquerque, NM 87185-1187 USA
Y. Maron and E. Stâmbulchik
Weizmann Institute of Science, Rehovot, Israel, 76100

We are using time- and space-resolved visible spectroscopy to measure applied-B ion diode dynamics on the 20 TW Particle Beam Fusion Accelerator II. Doppler broadening of fast Li atoms, as viewed parallel to the anode, is used in a charge-exchange model to obtain the Li^+ ion divergence within 100 μm of the anode surface. The characteristic Stark/Zeeman shifts in spectra of alkali neutrals or singly-ionized alkaline-earths are used to measrue the strong electric (10^9 V/m) and magnetic (~6 T) fields in the diode gap. Large Stark shifts within 0.5 mm of the anode indicate the LiF emits with a finite field threshold rather than with Child-Langmuir-type emission, and the small slope in the electric field indicates an unexpected build-up of electrons near the anode. In the diode gap, we aim to unfold fields to quantify the time-dependent ion and electron space-charge distributions that determine the ion beam properties. Observed electric field non-uniformities give local beam deflections that can be comparable to the total beam microdivergence. We are implementing active laser absorption and laser-induced fluorescence spectroscopy on low-density Na atoms injected into the diode gap prior to the power pulse. The small Doppler broadening in the Na spectra should allow simultaneous electric and magnetic field mapping with improved spatial resolution.

INTRODUCTION

Driving Inertial Confinement Fusion (ICF) targets with light ions in a pulsed-power accelerator requires efficient electrical power conversion into an appropriate-species ion beam of low divergence. This conversion is under study at Sandia in high-power applied-B ion diodes. We are using spectroscopic techniques to probe the physics of diode anode (A) and cathode (K) processes, and the AK gap space-charge distributions, on a 20 TW PBFA II Li^+ ion diode. The Stark shift of low-density excited neutrals in the AK gap is used to obtain the time- and 2-D-space-resolved electric field, which can then yield the electron and ion space-charge densities. This powerful non-perturbing technique [1] allows direct study of the diode gap charge dynamics that determine the limiting beam power density that can be delivered to an ICF target.

Previously-reported measurements [2] have described electric field profiles $E(x,t)$ in a barrel-geometry ion diode as a function of time t and the distance from the anode x. These profiles were compared with those generated by a fully-3-D, idealized particle-in-cell (PIC) simulation code [3]. Good agreement between simulation and experiment was seen early in the beam pulse, but a growing discrepancy within ~10 ns of the ion beam start showed that important non-ideal effects were missing from the simulation. Our goal is to measure, understand, and control these non-ideal effects to increase the ion beam brightness and ensure reliable scaling for a high-gain ICF driver.

MEASUREMENT USING GAP ATOMS

As described in detail elsewhere [4], an array of lens-coupled fiber optics is used to collect AK gap optical emission from ~2 mm diameter cylindrical lines-of-sight and transport that light to remote multiplexed spectrographs, where the spectra are streaked and recorded on film. The 3×6 fiber arrays can be oriented with the longer dimension across the AK gap (x direction) to resolve the $E(x,t)$ profiles, or oriented parallel to the anode surface (the azimuthal direction ϕ in a barrel-geometry or extraction-geometry ion diode) to resolve $E(\phi,t)$ non-uniformities. An extremely useful feature in the emission spectra is Stark-shifted 2s-2p emission from ~10^{12} cm^{-3} Li atoms in the ~10 MV/cm AK gap electric field. The calculated and measured Stark shifts of these non-Rydberg transitions offer a previously-untested regime for advancing Stark effect and basic atomic physics calculations [5]. The Li atoms are observed to have several-keV Doppler

broadening energies parallel to the anode surface, and move away from the anode across the AK gap with typically 10 keV energies. The fast Li atom energies and the absolute Li atom density seen appear to be due to Li atom production via charge exchange of the Li^+ ion beam in a few monolayers of desorbed anode impurities. Only about 5% of the Li^+ beam ions undergo charge exchange events to make the low-density Li atoms we observe, so this process is not expected to contribute significantly to impedance loss [6].

SOURCE & NEAR-SOURCE RESULTS

These experiments used a passive LiF-coated anode that emits Li^+ ions when subjected to ~5-10 MV/cm electric fields. It is important to know the beam microdivergence generated by the ion emission source, since the total Li^+ beam microdivergence of typically 25 mrad after acceleration to 9 MeV is at least twice what is needed for efficient ICF target drive. It is difficult to spectroscopically observe directly the Li^+ ions because their closed-shell atomic structure puts populated-transition wavelengths into the extreme vacuum ultra-violet. Instead, we use the charge-exchange model of fast Li atom production to infer the Li^+ ion beam microdivergence very close to the anode surface.

The small fraction of Li^+ ions undergoing a charge exchange event in a thin desorbed impurity layer can be modeled. We assume self-consistently that the charge exchange layer thickness is much larger than the few-micron scale size of charge clumping or conductor surface roughness needed even to account for all the final beam microdivergence being acquired near the anode surface. The velocity distribution of the Li^+ ions at the charge-exchange layer is then essentially transferred to the Li atoms, and the angular spread in Li^+ ion velocities can be obtained from the Doppler broadening of Li atom emission viewed parallel to the anode surface. Geometrical path length effects in the charge-exchange layer give typically less than 20% correction of the atom velocity full-width-at-half-maximum (FWHM) to obtain the incident ion velocity FWHM. Using this technique, we find that typically at most about half the final beam microdivergence is acquired in the immediate ion source vicinity. The remainder may be due to instabilities [7] or non-uniformities [8].

Another interesting result is the measurement of electric field at ~1/2 mm from the LiF anode, showing field strength much larger than the space-charge-limited (SCL) value [2]. For even moderately-uniform ion emission this result would require the LiF surface has a non-zero field value during intense ion current emission, in contrast with the zero-field SCL condition. Our measurements show that, even allowing for ion space-charge effects, the anode electric field is typically 7-10 MV/cm in the early phase of the ion beam. This field-threshold emission is consistent with earlier theoretical ideas on ion emission from LiF in strong electric fields and intense electron bombardment [9]. Later in the power pulse, Li atom emission is observed with no Stark shift near the anode while the onset of impurity ion lines is seen, indicating plasma does form non-uniformly over the anode at about the time that impurity C,O, and H ions are significantly contaminating the Li^+ beam [10]. We are investigating electron stimulated and thermal impurity desorption and ionization as a mechanism for this beam purity loss and diode impedance loss.

AK GAP RESULTS

Further insight has been gained on the surprising observation [2] of approximately-uniform $E(x)$ in the first few mm away from the anode surface. Previous theoretical ideas and simulation results had the ion space-charge dominating the electron space-charge near the anode, so that from Gauss' law the electric field should have increased sharply with distance from the anode, until the dense part of the electron sheath was encountered some distance across the AK gap. A nearly-flat or falling $E(x)$ profile near the anode (see Figure 1) implies an electron build-up there comparable to the ion space-charge. However, such extensive electron diffusion across the AK gap is usually intuitively associated with extreme ion currents, which we do not observe. As well, it is difficult to maintain large average electron density in the near-anode region unless most electrons there are moving essentially along the magnetic field.

We have shown that the flat near-anode $E(x)$ profiles actually give predicted ion current densities very consistent with what is observed. An integral expression obtained by one of us (MPD) using flux conservation and pressure balance gives implicitly the ion (mass M, charge q) cur-

rent density J_i across a physical AK gap d that is reduced by virtual cathode motion to a dynamic gap g, in terms of $E(x)$, the normalized electric potential $\tilde{\Phi}(x) \equiv \Phi(x)/V$ associated with the electric field ($\tilde{\Phi}(0) = 1, \tilde{\Phi}(g) = 0, \tilde{\Phi}'(g) = 0$), and the magnetic field at the virtual cathode B_C, as (in Gaussian units)

$$\overline{B_o}d = \int_0^g [B_c^2 + E^2(x) + \alpha J_i(1 - \sqrt{1 - \tilde{\Phi}(x)})]^{1/2} dx ,$$

with $\overline{B_o}d$ the average vacuum magnetic flux in the AK gap and $\alpha \equiv 8\pi\sqrt{(2MV)/q}$.

Our $E(x)$ profiles cannot be measured accurately out near the virtual cathode position because of the Li neutral time-of-flight delay. However, by simply assuming constant electron density beyond our largest-x measurement, where E is approaching zero, we can continue $E(x)$ out to $x=g$ and calculate J_i and g self-consistently. Figure 1 illustrates typical $E(x)$ data and the constant-density extrapolation. The calculated J_i of

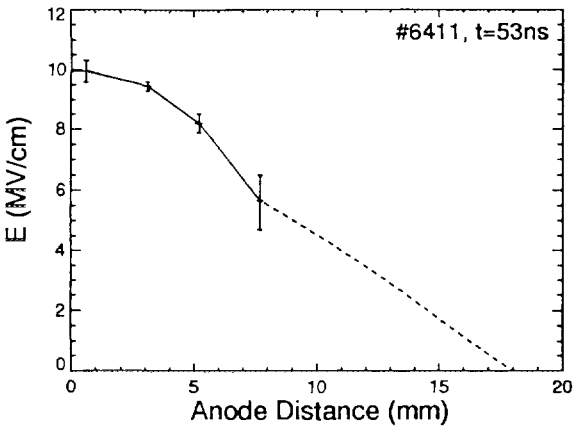

Fig. 1. Measured PBFA II diode electric field profile $E(x)$ with constant-density extrapolation (dashed).

0.9 kA/cm^2 agrees well with the average current density measured by filtered Faraday cups and an ion magnetic spectrometer. These results give us confidence in the data interpretation, but the remaining discrepancy with simulation charge distributions indicates additional physics may need to be included in the simulations.

Detailed $E(x,\phi)$ time evolution has been measured in the diode gap using up to 18 lines-of-sight in the 3×6 fiber array. Figure 2 shows a sequence of 2-ns-averaged $E(x,\phi)$, illustrating the large variations and non-uniformities as a function of ϕ. In an ideal diode, $E(\phi)$ at fixed x would

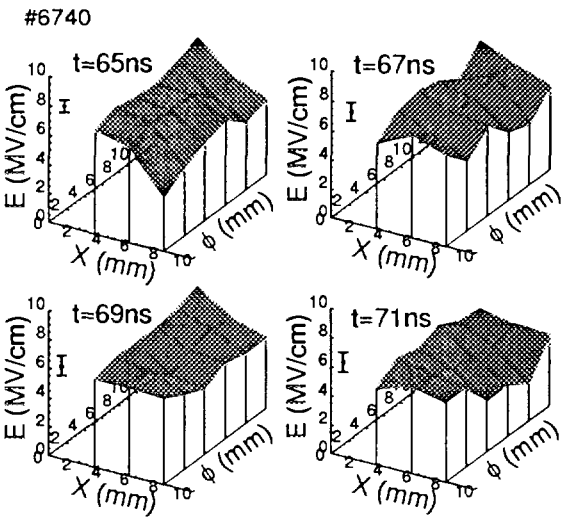

Fig. 2. Measured 2-D-resolved PBFA II diode electric field as a function of distance across (x) and along (ϕ) the AK gap, starting 5 ns after peak Li^+ beam power. Typical error bars are shown.

be constant during our time-averaging window. The experimental non-uniformities indicate fluctuations of net charge density over space and time, possibly caused by intermittent anode or cathode plasma phenomena.

The non-uniform $E(\phi)$ implies azimuthal clumping of potential and existence of electric field components E_ϕ transverse to the direction of primary beam acceleration. These E_ϕ components can deflect the beam and impair the final focus quality on target. We have done high-precision $E(x,\phi)$ measurements as shown in Figure 1 to obtain estimates of $E_\phi(x)$ and the associated RMS local beam deflection angles. $E(x)$ at two adjacent azimuths A and B are used to calculate the potentials $\Phi_{A,B}(x)$ by assuming self-consistently that $E_x \sim E$. Since the anode is a constant-potential conductor and induced $\frac{\partial B}{\partial t}$ potentials are negligible, $E_\phi(x)$ between A and B can be estimated as $-(\Phi_A - \Phi_B)/d_{AB}$ (where is $d_{AB} \sim 2$ mm is the azimuthal distance between A and B). The E measurement uncertainty needs to be better than ±5% to obtain statistically meaningful results for E_ϕ. We have done extensive uncertainty characterization of our E measurement technique to verify the size of our error bars [11]. Preliminary results of unfolds are shown in Figure 3. Short-lived transverse fields increasing up to several MV/cm with distance from the anode indicate azimuthal charge clumping that can give ~25 mrad RMS beam deflections, comparable to the typical total beam microdivergence. The mechanism for these charge nonuniformities

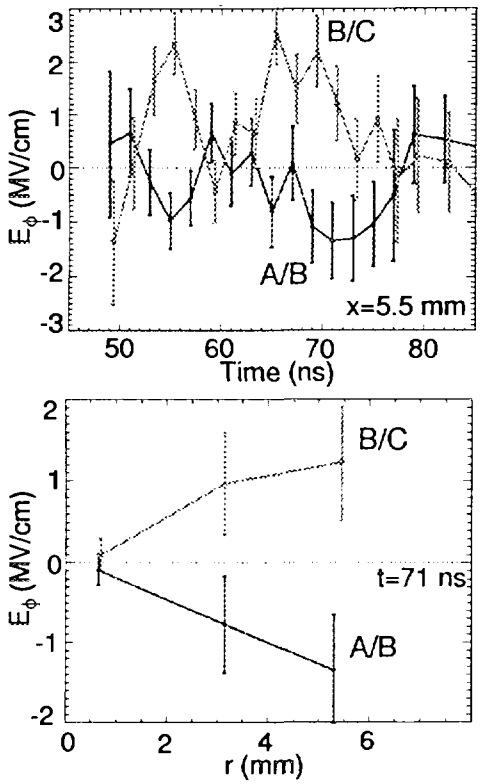

Fig. 3. Preliminary unfolded E_ϕ components from a PBFA II experiment, at azimuths A,B and B,C: a) at fixed position x, and b) at fixed time t. Ion beam onset is at t=41 ns.

needs to be understood.

ACTIVE SPECTROSCOPY

While much has been learned by viewing the conveniently-occurring Li atom emission, this passive spectroscopy is limited by the ~30 ns atom time-of-flight across the AK gap, the large Doppler broadening of the fast Li atoms, and the line-of-sight integration. We are implementing an Active Spectroscopy Probe (ASP) by injecting ~5×10^{12} cm^{-3} Na atoms into the diode AK gap just prior to the experiment, and using saturated laser-resonance-fluorescence or absorption spectroscopy to obtain a detailed Stark-Zeeman Na I 3s-3p pattern with full 3-D space and time resolution [12]. As shown in Figure 4, the information content in the low-Doppler-broadening Na atom emission pattern can give much better electric and magnetic field measurement than from the fast Li atoms, yielding the charge and magnetic flux information needed for understanding of actual ion diodes. Initial experiments [13] with the laser-driven low-density Na atom source and collection optics are promising.

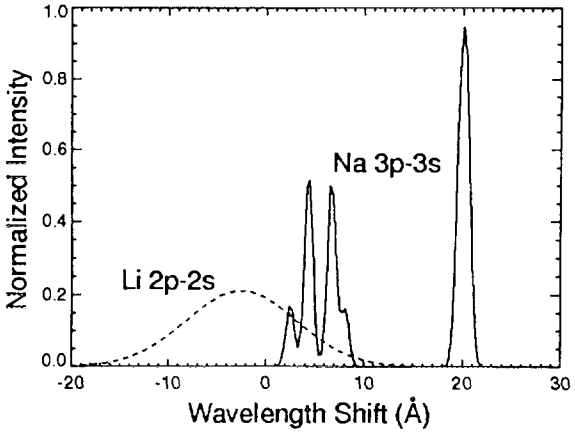

Fig. 4. Comparison of calculated Stark/Zeeman-shifted resonance-line emission for comparable densities of naturally-occurring fast Li atoms (dashed) and actively-injected Na atoms (solid). Calculation used 6 MV/cm and 6 T crossed electric and magnetic fields.

We are grateful to the PBFA II operations crew and D.F. Wenger for technical assistance, and to D.L. Cook, R.J. Leeper, and J.P. Quintenz for support. Funding for this work has been provided by the U. S. Department of Energy under Contract DE-AC04-94-AL85000.

[1]Y. Maron, et al., Phys. Rev. Lett. 57, 699 (1986), Phys. Rev. A. 36, 2818 (1987).

[2]J.E. Bailey, et al., Phys. Rev. Lett. 74, 1771 (1995).

[3]T.D. Pointon et.al., Phys. Plasmas 1, 429 (1994).

[4]J. Bailey, et al., Rev. Sci. Instr. 61, 3075 (1990).

[5]J.E. Bailey, in *Proc. 7th Int. Workshop on Atomic Physics for Ion-Driven Fusion, Madrid, Spain*, October 16-20, 1995. To be published in Laser & Particle Beams.

[6]M.P. Desjarlais, J. Appl. Phys. 66, 2888 (1989).

[7]M. P. Desjarlais et al., Phys. Rev. Lett. 67, 3094 (1991).

[8]S.A. Slutz, Phys. Fluids B 4, 2645 (1992).

[9]T. A. Green et al., Sandia National Laboratories report SAND95-1794 (available from NTIS).

[10]T. A. Mehlhorn et al., in *Proc. 10th Int. Conf. on High Power Particle Beams, San Diego, CA*, 1994 (NTIS PB95-144317), p. 53.

[11]J.E. Bailey, et al., in *Proc. 13th Topical Conf. on High-Temperature Plasma Diagnostics, Monterey, CA*, May 13-17, 1996. To be published in Rev. Sci. Instr.

[12]B.A. Knyazev, et al., in *Proc. 9th Int. Conf. on High Power Particle Beams, Washington, DC*, 1992 (NTIS PB92-206168), p. 1043.

[13]C.-H. Hong, et al., in Ref. 11.